Cell, Vol. 95, 409–417, October 30, 1998, Copyright ©1998 by Cell Press

Structure of the Hemagglutinin Precursor Cleavage Site, a Determinant of Influenza Pathogenicity and the Origin of the Labile Conformation

Jue Chen*#, Kon Ho Lee,‡# David A. Steinhauer,§# David J. Stevens,§ John J. Skehel,§ and Don C. Wiley*†‡‖
*Department of Molecular and Cellular Biology
Harvard University and
†Howard Hughes Medical Institute
Cambridge, Massachusetts 02138
‡Laboratory of Molecular Medicine
Department of Medicine
The Children's Hospital and
†Howard Hughes Medical Institute
Boston, Massachusetts 02115
§National Institute for Medical Research
The Ridgeway
Mill Hill, London NW7 1AA
United Kingdom

Summary

The membrane fusion potential of influenza HA, like many viral membrane-fusion glycoproteins, is generated by proteolytic cleavage of a biosynthetic precursor. The three-dimensional structure of ectodomain of the precursor HA0 has been determined and compared with that of cleaved HA. The cleavage site is a prominent surface loop adjacent to a novel cavity; cleavage results in structural rearrangements in which the nonpolar amino acids near the new amino terminus bury ionizable residues in the cavity that are implicated in the low-pH-induced conformational change. Amino acid insertions at the cleavage site in HAs of virulent avian viruses and those of viruses isolated from the recent severe outbreak of influenza in humans in Hong Kong would extend this surface loop, facilitating intracellular cleavage.

Introduction

The influenza virus hemagglutinin biosynthetic precursor HA0 is a glycoprotein held in the viral membrane by a transmembrane anchor sequence near its COOH terminus. Its cleavage results in the formation of the two disulfide-linked subunits HA1 and HA2, eliminating an arginine residue, R329, that separates them in the precursor (reviewed in Wiley and Skehel, 1987). The newly created amino terminal of HA2 is a nonpolar sequence called the fusion peptide. Cleavage is essential for infectivity (Klenk et al., 1975; Lazarowitz and Choppin, 1975) as it activates the potential of the HA to undergo a low-pH-induced, irreversible conformational change in endosomes required for viral entry by membrane fusion (Maeda and Ohnshi, 1980; Skehel et al., 1982; Wiley and Skehel, 1987; Godley et al., 1992). Intracellular cleavage correlates with virus pathogenicity (reviewed in Webster and Rott, 1987; Klenk and Rott, 1988; Klenk and Garten, 1994); its inhibition presents a target for antiviral agents (Garten et al., 1989; Stieneke-Grober et al., 1992).

The conformation of the precursor HA0 is stable at low pH, but cleaved HA is apparently metastable (Bullough et al., 1994). Once cleaved, HA is sensitive to pH, undergoing an irreversible conformational change (Skehel et al., 1982) at the low pH of endosomes that is required for membrane fusion. The low-pH-induced conformation melts at a higher temperature than the original conformation (Ruigrok et al., 1988) and is achieved spontaneously at neutral pH by soluble HA2 expressed in bacteria, suggesting that it is the lowest energy conformation (Chen et al., 1995; Carr et al., 1997). The low-pH-induced conformational change is a dramatic refolding of HA2 that both projects the N-terminal fusion peptide 100 Å to the end of a long coiled-coil rod (Carr and Kim, 1993; Bullough et al., 1994) and relocates the C-terminal anchor, by a fold-back mechanism, to the same end of the rod-shaped molecule (Bullough et al., 1994). In the process of membrane fusion, this conformational change brings the target membrane–inserted fusion peptide near the transmembrane sequence anchored in the viral membrane (Weissenhorn et al., 1997). A rod-like molecular shape with membrane attachments all at one end has also been found in ectodomain fragments of HIV-1 gp41 (Chan et al., 1997; Tan et al., 1997; Weissenhorn et al., 1997) and the complex of v- and t-SNAREs that fuses synaptic vesicles (Hanson et al., 1997; Weber et al., 1998). The structure of HA0 reported here addresses both the origin of the labile HA conformation and its sensitivity to low pH.

Mammalian and apathogenic avian influenza virus strains cause anatomically localized infections as a result of the restricted range of cells secreting a protease that can cleave the HA0 precursor extracellularly (Klenk et al., 1993). Highly pathogenic avian strains, however, are cleaved by a family of more widespread intracellular proteases, resulting in systemic infections. This difference in pathogenicity correlates with structural differences at the HA0 cleavage site: pathogenic strains have inserts of basic amino acids at the site or other sequence modifications in its vicinity (Webster and Rott, 1987; Klenk and Rott, 1988; Klenk and Garten, 1994). The HA0 structure reported here defines the precursor cleavage site of a human influenza hemagglutinin.

Recombinant HA0 was expressed with a mutated cleavage site (R329Q) and trypsinized off the surface of CV-1 cells to form a crystallizable, soluble ectodomain (R329Q $HA0_s$). Biochemical evidence is presented that the mutant $HA0_s$ undergoes the same low-pH-induced conformational change after cleavage as wild-type HA0. The X-ray structure of the mutant $HA0_s$ shows how variation in the structure of the precursor cleavage site leads to variation in the pathogenicity of viruses. Comparison with cleaved BHA provides new evidence for the origin of the metastability and sensitivity to low pH of the conformation of HA formed after HA0 cleavage.

‖To whom correspondence should be addressed (e-mail: dcwadmin@crystal.harvard.edu).
#These authors contributed equally to the work.

Results

Biochemical Characterization of Mutant R329Q HA0

The precursor HA0 is susceptible at or near the cleavage site (Arg-329) to numerous proteases. To prepare soluble HA0 ($HA0_s$), which requires proteolytic removal of a membrane anchor sequence, we constructed a mutant in which arginine 329 was replaced by glutamine, R329Q, to prevent tryptic cleavage at the precursor site, and a 14 residue sequence containing multiple protease recognition sites (Germino and Bastia, 1984) was inserted immediately before the transmembrane anchor sequence. Efforts to prepare soluble trimers of HA0 by secreting $HA0_s$ monomers failed to generate trimeric molecules efficiently. We produced a recombinant vaccinia virus containing this mutant HA gene and released soluble R329Q mutant HA0 from the membranes of recombinant-infected CV-1 cells by digestion with trypsin.

Biochemical and immunological data indicate that soluble R329Q $HA0_s$ is closely similar to wild-type HA0. Both molecules are trimeric as judged by sedimentation (Figure 1A) and are antigenically indistinguishable in their reactivities with a panel of monoclonal antibodies at neutral pH or following incubation below fusion pH (pH 5.0). The protease bromelain cleaves HA0 at G330 instead of R329 (Steinhauer et al., 1995). HA cleaved in this way is not fusion active (because HA2 lacks Gly-1) but nevertheless undergoes changes in conformation characteristic of those required for membrane fusion activity. On incubation at fusion pH, bromelain-cleaved R329Q $HA0_s$ aggregates and becomes susceptible to trypsin digestion as observed earlier for wild-type HA (e.g., Figure 4 in Skehel et al., 1982). The products of digestion can be separated by sucrose density gradient centrifugation into aggregated HA2 and a soluble HA1 fraction that reveals cleavages within HA1 at Lys-27 and Arg-224 in both wild-type and R329Q HA (cf. Figure 1B to Figure 4 in Skehel et al., 1982). By contrast, uncleaved R329Q $HA0_s$, even after incubation at pH 5.0, sediments as a protease-resistant trimer.

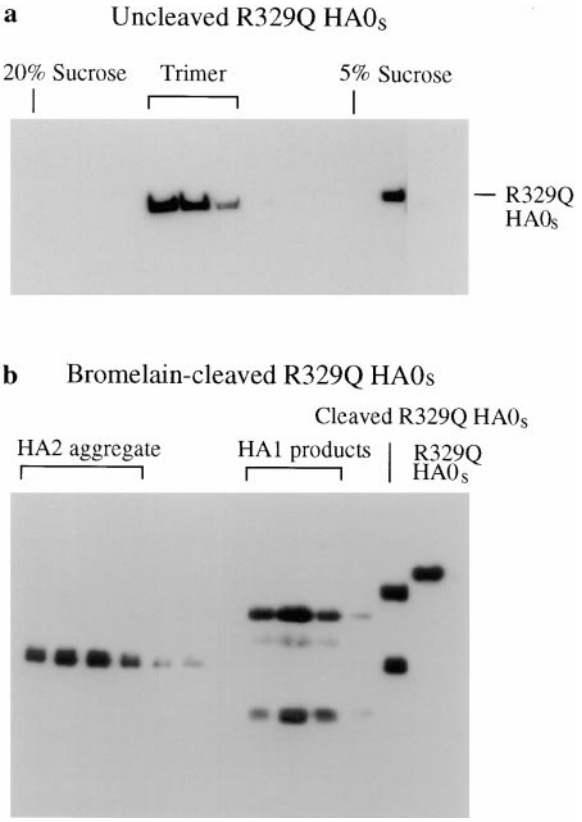

Figure 1. Protease Susceptibility of Bromelain-Cleaved R329Q $HA0_s$ after Incubation at Low pH

Soluble R329Q $HA0_s$ (membrane anchor removed by trypsin) was digested with bromelain (1 mg/ml, 50 mM β-mercaptoethanol, 10 mM Tris [pH 8.0], 37°C, 2 hr), producing HA2 without the NH2-terminal glycine (Steinhauer et al., 1995). Bromelain-cleaved and uncleaved preparations were incubated at pH 5.0 for 10 min at 37°C, and after neutralization, digested with trypsin (10 mg/ml, 10 mM Tris [pH 8.0], 37°C, 10 min). The products of digestion were separated by sucrose density gradient centrifugation (5.%–20.%) and detected in fractions from the gradients by SDS-PAGE and immunoblotting using an anti-HA rabbit serum. HA0 markers (right lane) are soluble R329Q $HA0_s$ (membrane anchor removed by trypsin).

Precursor HA0 Structure

The Cleavage Site

The structure of soluble R329Q $HA0_s$ was determined by X-ray crystallography and refined to 2.8 Å resolution (R_{cryst} = .302, R_{work} = .224) with crystals grown at pH 7.5. The main chain of only 19 residues, in a sequence bracketing the cleavage site, is located differently in uncleaved R329Q $HA0_s$ relative to BHA (solid bonds in Figures 2A and 2B; yellow in Figure 2C) (Wilson et al., 1981; Weis et al., 1990); the remaining residues are essentially superimposable (rms deviation = 0.49 Å for 472 residues). The cleavage site 19 residues, (323–328 of HA1, Q329, and 1–12 of HA2), form a nearly circular loop in R329Q $HA0_s$ (solid bonds in Figure 2A) that projects the 8 residues that immediately surround the cleavage site, from residue 327 of HA1 to residue 5 of HA2, away from the surface of the molecule into solvent (arrow in Figure 2C). In R329Q $HA0_s$, HA2 residues 12 to 6 lie against the molecule, extending down along the surface and covering the interchain disulfide bond between Cys-14 of HA1 and Cys-137 of HA2; in cleaved BHA, they point toward the long α helix of HA2 and the trimer axis (Figures 2C and 2D). An oligosaccharide is attached at residue 22 of HA1, just 14 Å away from the cleavage point (Figure 2C).

A Surface Cavity in HA0

There is a deep cavity in R329Q $HA0_s$ adjacent to the cleavage site loop (arrow in Figure 3A), which is filled in cleaved BHA (Figure 3B) by HA2 residues 1–10, a nonpolar segment of the fusion peptide. The cavity contains ionizable residues, including aspartic acids 109 and 112 on the long α helix of HA2 and histidine 17 of HA1 (Figure 3C). As a consequence of cleavage, these three ionizable residues are buried without pairing to other ions; the aspartates (HA2 residues 109 and 112) form five hydrogen bonds with the five main-chain amide groups of residues 2–6 of the fusion peptide of HA2 (Weis et al., 1990), and histidine 17 forms a hydrogen bond from Ne2 through a water to the carbonyl oxygen of HA2 residue 10 (Figure 3D). Two C-terminal residues

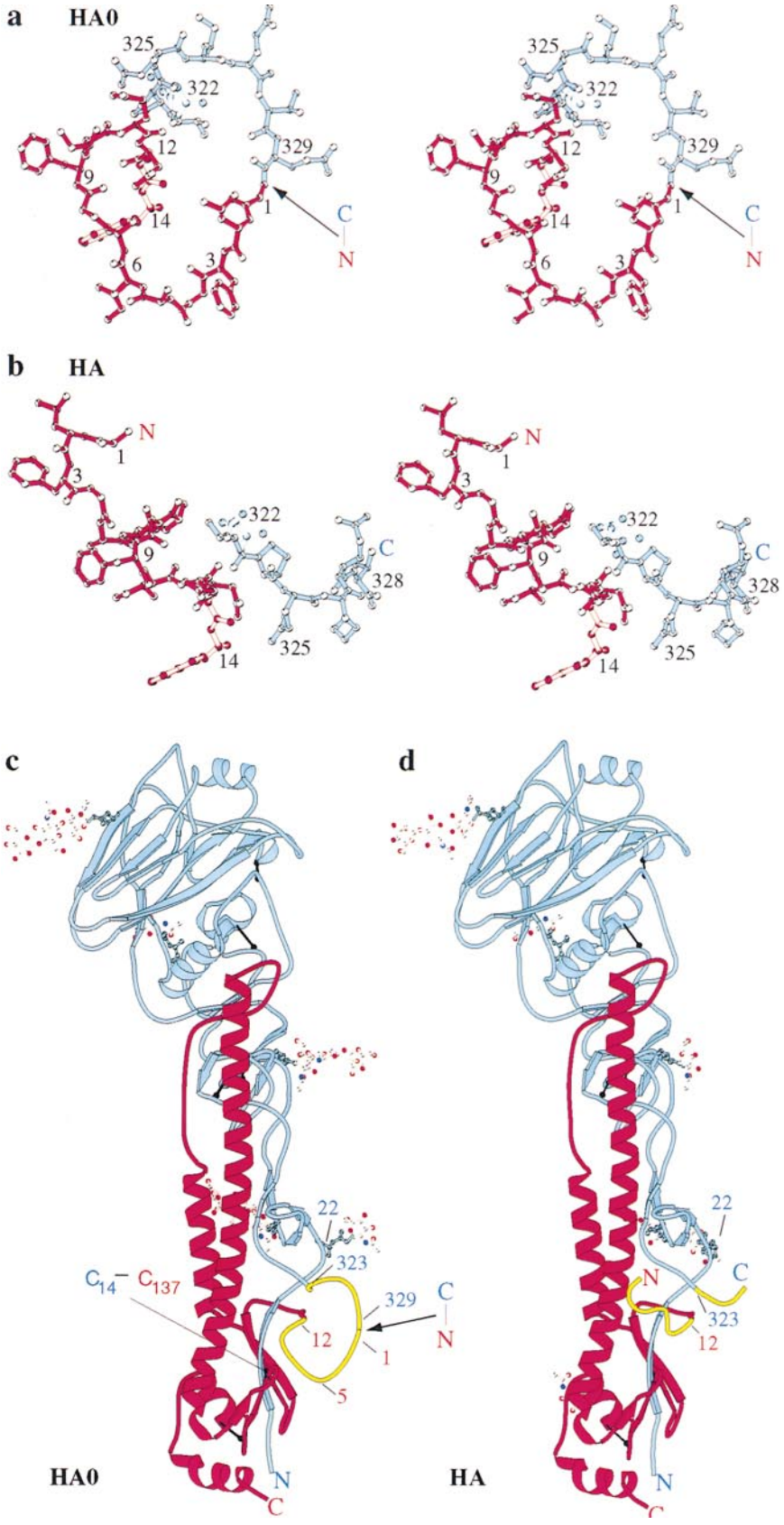

Figure 2. Structure of the Precursor (R239Q $HA0_s$) Cleavage Site before and after Cleavage

(A) Stereo diagram of residues 322–329 and 1–14 of the HA1 and HA2 parts of R239Q $HA0_s$. Residues 323 HA1 to 12 HA2 relocate after cleavage (solid bonds: HA1, blue; HA2, red); residues 322 and 13–14 (open bonds) occupy the same location before and after cleavage. (B) Stereo diagram of the same residues (and color code) as in (A) after cleavage (Wilson et al., 1981; Weis et al., 1990). Newly created termini are 22.5 Å from each other.

(C) R329Q $HA0_s$ monomer. Cleavage site at arrow. Residues that relocate, 323–329 HA1 and 1–12 HA2, are colored yellow; HA1, blue; HA2, red.

(D) Cleaved HA monomer. Figure prepared with MOLSCRIPT (Kraulis, 1991).

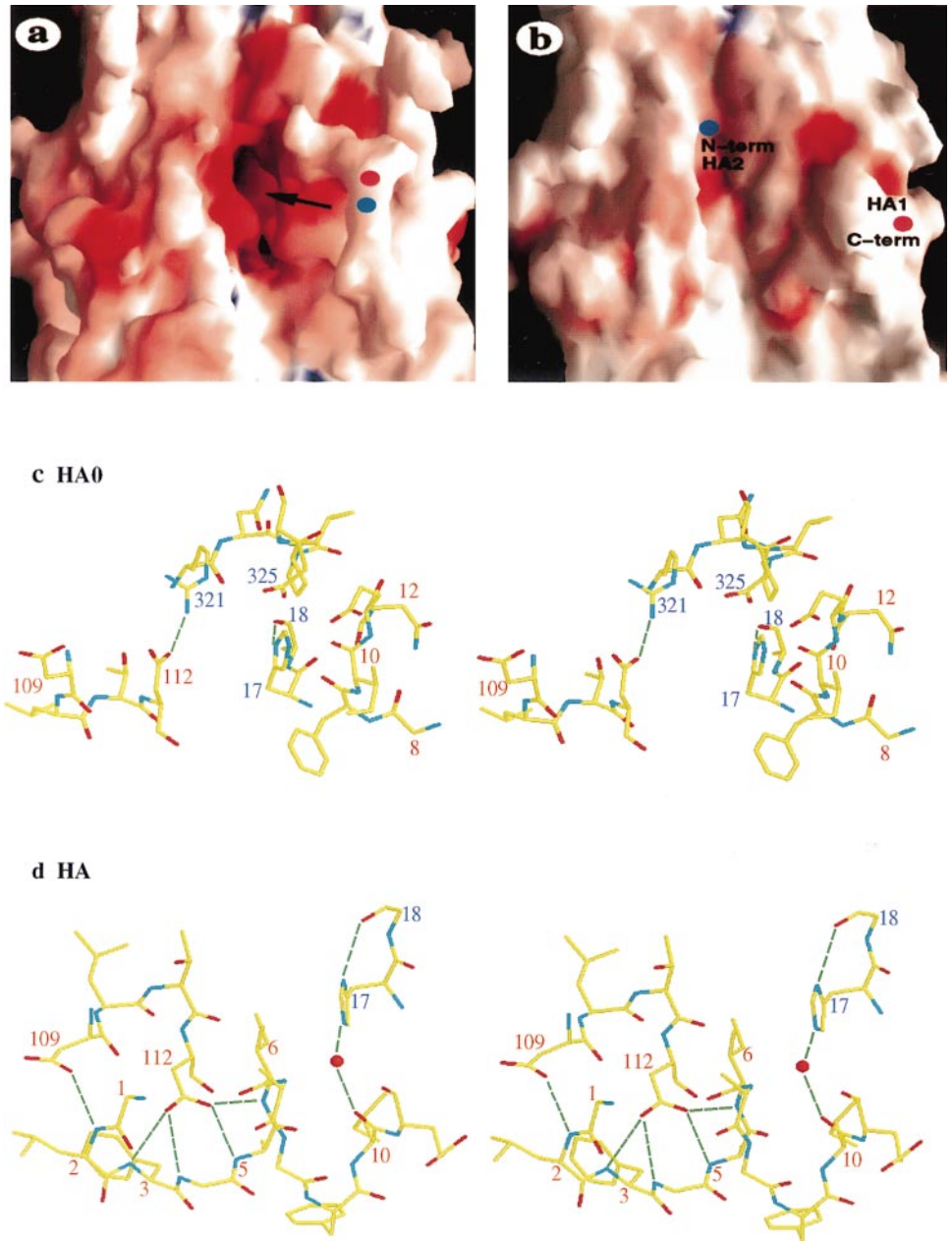

Figure 3. A Surface Cavity in HA0 Adjacent to the Cleavage Site Is Filled by the Fusion Peptide after Cleavage

(A) Electrostatic surface potential of R329Q $HA0_s$ trimer with cavity at arrow. Cleavage site is on the loop between the labeled (red and blue dots) HA1 C terminal and HA2 N terminal. The cavity surface is approximately 10 Å wide and 30 Å long.

(B) Cleaved BHA surface showing separation of the newly created termini. Negative electrostatic potential, red; positive, blue. 797 $Å^2$ of solvent-accessible surface area of the R329Q $HA0_s$ cavity and 1380 $Å^2$ of the fusion peptide are buried as a result of the cleavage and subsequent rearrangement shown in Figures 2 and 3.

(C) Stereo diagram of R329Q $HA0_s$ showing the environment of Asp-109 and -112 (HA2) and His-17 (HA1) that are buried in cleaved HA.

(D) Stereo diagram of cleaved HA showing the buried environment of Asp-109 and -112 (HA2) and His-17 (HA1). (Dashed lines are potential hydrogen bonds.) Figure prepared with GRASP (Nicholls et al., 1991) and RasMol (Collaborative Computational Project, 1994).

of HA1 move out of the top part of the cavity after cleavage: Glu-325 (HA1) and the side chain of Arg-321 (HA1) that was hydrogen bonded to Asp-112 (HA2) in HA0 both move away from the cavity into solution. All of the ionizable residues in this cavity (HA1: H17; HA2: D109, D112, K117) have been identified as affecting the pH at which membrane fusion occurs in mutants selected to fuse at higher pH (reviewed in Wiley and Skehel, 1987; Steinhauer et al., 1992). Mutants at Asp-112 are also resistant to some fusion inhibitors (Hoffman et al., 1997).

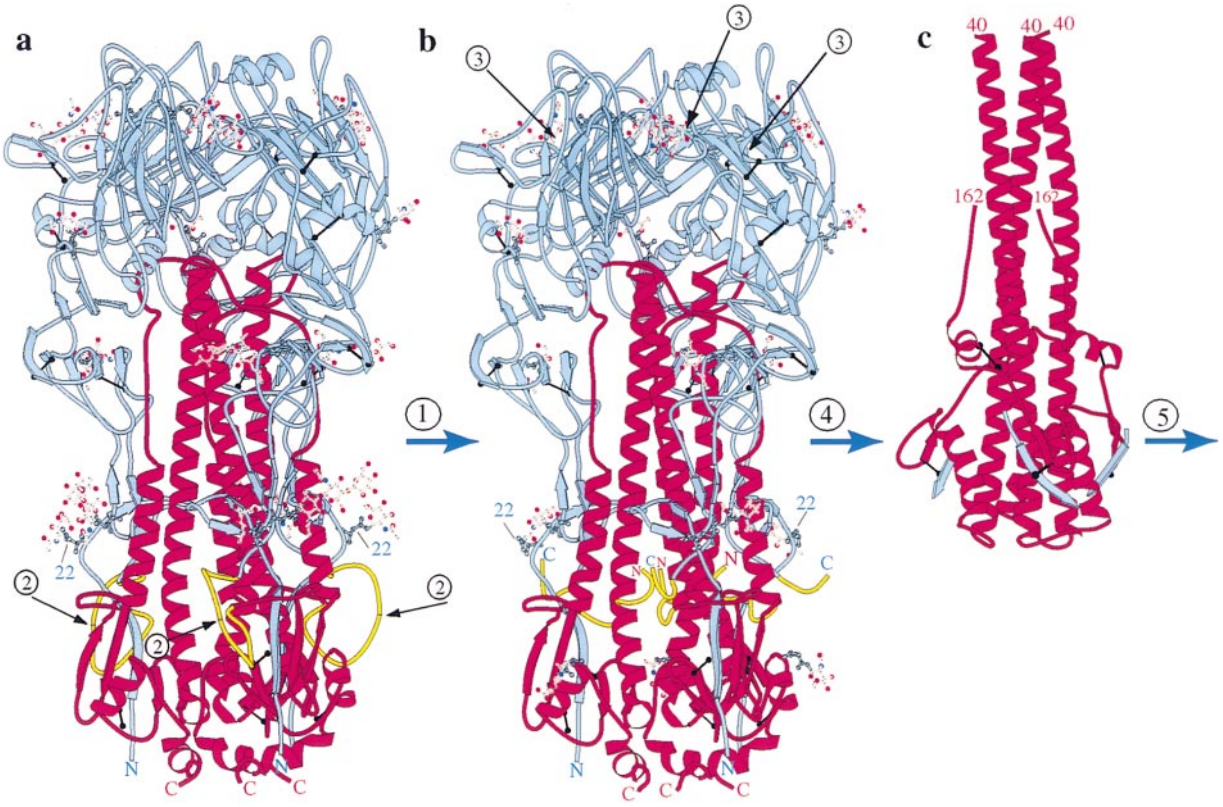

Figure 4. Three Conformations of the HA Trimer

(A) Uncleaved precursor R329Q $HA0_s$. Arrow 2 marks cleavage sites and adjacent cavities in each monomer. Residues 323 of HA1 to 12 of HA2 are yellow. Oligosaccharides shown as balls and sticks; oligosaccharide at Asn-22 of HA1 is labeled.

(B) Cleaved BHA (Wilson et al., 1981). Receptor binding sites marked with arrow 3 (Weis et al., 1988).

(C) Low-pH-induced conformation of thermolysin-solubilized TBHA2 (Bullough et al., 1994). HA1, blue; HA2, red. Disulfide bonds are black lines. Figure prepared with MOLSCRIPT (Kraulis, 1991).

Three HA Conformations Have Been Determined by X-Ray Crystallography

Three conformations of HA have now been defined structurally (Figure 4). These conformations and the interconversion events are potential targets for antiviral compounds. The conversion of HA0 to the cleaved conformation might be blocked by inhibiting the cleavage enzymes (arrow 1 in Figure 4) (Garten et al., 1989; Stieneke-Grober et al., 1992) or by the binding of an inhibitor into the cavity revealed in the R329Q $HA0_s$ structure (arrow 2 in Figure 4) to prevent the insertion of the fusion peptide. Blocking the conserved receptor binding site (arrow 3 in Figure 4) (e.g., Watowich et al., 1994 and references therein) or the low-pH-induced conformational change (arrow 4 in Figure 4) are also strategies that have been suggested (see Godley et al., 1992 and e.g., Bodian et al., 1993). Interfering with a transient structure during refolding as demonstrated for HIV-1 gp41 (Wild et al., 1994) or with the membrane fusion process itself are also possibilities (arrow 4 or 5 in Figure 4). Compounds that inhibited the functions of the target-rich HA in these ways would add to the collection of anti-influenza drugs provided by the M2 proton channel inhibitors amantadine and rimantidine (Hay, 1989) and the anti-neuraminidase (NA) compounds designed with the aid of the NA structure (von Itzstein et al., 1993) and may contribute to drug combination therapies effective against the development of resistance.

Discussion

Precursor Cleavage

The proteases responsible for cleavage of HA0 in influenza infections of humans are secreted by cells of the respiratory tract or by coinfecting bacteria or mycoplasma or may be produced in inflammatory responses to infection (Klenk and Rott, 1988; Klenk and Garten, 1994). A major candidate protease is tryptase Clara, which is produced by Clara cells of the bronchiolar epithelium (Kido et al., 1992). It is specific for the sequence Q/E-X-R found at the cleavage site of the $HA0_s$ of the three known antigenic subtypes of human influenza. No protease has been identified for the majority of influenza viruses (15 antigenic subtypes) that cause enteric and respiratory infections in waterfowl. It is possible that a requirement for the Q/E-X-R recognition sequence for replication in the human respiratory tract selects against infections by avian viruses.

The HAs of the avian viruses that caused the recent outbreaks of human influenza in Hong Kong contained

a five-residue insertion of basic amino acids at the site of cleavage (Subbarao et al., 1998). Such insertions, which may result from slippage of the RNA polymerase at a particular region of RNA structure (Perdue et al., 1997), are observed exclusively in the HAs of the H5 and H7 subtypes, and their presence correlates with virulence for chickens (Webster and Rott, 1987; Klenk and Rott, 1988; Klenk and Garten, 1994). Cleavage in these cases is intracellular, and the proteases involved have been identified as furin and other subtilisin-like enzymes involved in the posttranslational processing of hormone and growth factor precursors. The furin recognition sequence R-X-R/K-R is a frequent insertion at the HA0 cleavage sites of H5 and H7 HAs, and both the wide tissue distribution of this enzyme and the efficiency of intracellular cleavage compared to opportunistic extracellular cleavage appear to contribute to the widespread and virulent systemic infections of these viruses (Webster and Rott, 1987; Klenk and Rott, 1988; Klenk and Garten, 1994).

Precursor Cleavage and Pathogenicity

The structure of R329Q $HA0_s$ revealed that the side chain of P-4 (Lys-326) is packed against the HA0 structure and would not be accessible for binding into an enzyme active-site recognition pocket as furins appear to require. This may explain why furin sites on HAs are always four-residue inserts. The structure of R329Q $HA0_s$ suggests that the insertion of 4 residues at the cleavage site will both project the protease recognition site, as a prominent bulge, into solution and expose the critical, inserted P-4 arginine to direct recognition by furin-like proteases. Similar structures may also be involved at the cleavage sites of membrane fusion glycoproteins of other viruses: paramyxoviruses such as measles, mumps, and respiratory synctial viruses; the filoviruses Ebola and Marburg; and retroviruses such as HIV-1 and Rous sarcoma virus all have furin recognition sites like intracellularly cleaved influenza HA0. This interpretation is consistent with the increased cleavability observed for HAs of two mutants that were selected by replication in tissue culture in the absence of extracellular proteases and that contained in-frame insertions near the cleavage site of 18 residues coded by 28S ribosomal RNA or 20 residues coded by the gene for influenza nucleoprotein (Khatchikian et al., 1989; Orlich et al., 1994), which would also be expected to project the cleavage site into solution.

Some H5 influenza strains lack an inserted furin recognition site but are still highly pathogenic. These viruses either lack an oligosaccharide at Asn-11 (Kawaoka et al., 1984) (the H5 subtype homolog of Asn-22 in X31 HA; Figures 2C and 3A) or contain basic amino acid substitutions at P-5 and P-6 (Webster and Rott, 1987; Ohuchi et al., 1989; Vey et al., 1992). The former observation is consistent with the proximity of this oligosaccharide to the cleavage site in R329Q $HA0_s$ (14 Å) (Figure 3A), which, as noted earlier (Kawaoka et al., 1984; Deshpande et al., 1987; Kawaoka and Webster, 1989), could influence the accessibility of a protease to the cleavage site. The structure of R329Q $HA0_s$ suggests that the substitutions made at P-5 and P-6, in the latter report, may perturb the structure of HA0 because those residues are not on the exposed loop. Such perturbations could cause an increase in the accessibility of the cleavage site. Site-specific mutant H3 subtype $HA0_s$s with increased cleavability are accounted for by the same mechanisms (Gething et al., 1989; Ohuchi et al., 1989).

The susceptibility of HA0 to cleavage correlates with pathogenicity both in avian infections and in the recent Hong Kong influenza outbreak in humans in which 6 of the 18 confirmed cases were fatal (WHO, 1998). The R329Q $HA0_s$ structure provides a structural explanation for the correlation of precursor cleavage with pathogenesis and supports the use of properties that influence cleavage as markers of virulence in the surveillance of influenza viruses.

Precursor Cleavage Activates the Potential for the Low-pH-Induced Conformational Change

What permits cleaved HA on virus to undergo a low-pH-induced irreversible conformational change, while the uncleaved precursor, HA0, does not? It seems possible from the structure of R329Q $HA0_s$ that the movement of the fusion peptide into the cavity in HA0, burying ionizable residues (Figure 3), may set a low-pH trigger. In that case, precursor cleavage would be required to set the pH trigger before the conformational change could be induced by low pH. Alternatively, it seems possible that the covalent bond per se that links HA1 to HA2 in HA0 might restrict the movement of the fusion peptide, preventing the extensive conformational refolding observed after low-pH treatment of the cleaved molecule (Figure 4).

The existence of HA0 molecules with insertions from 4 to 20 residues at the cleavage site (Webster and Rott, 1987; Klenk and Rott, 1988; Klenk and Garten, 1994) raises the question of why, with such long loops, the fusion peptide could not move into the HA0 surface cavity without cleavage, setting the presumptive pH trigger and becoming conformationally labile to low pH without precursor cleavage? The answer may be that the HA0 cavity is, in a sense, partially filled. Arg-321, Pro-324, and Glu-325 all need to move out of the top portion of the cavity (Figure 3C; residues above arrowhead in Figure 3A) before the fusion peptide will fit in. It seems likely that precursor cleavage allows these three HA1 residues to move away from their location in HA0 so that the N-terminal sequence can fill the cavity. As a consequence, the carboxyl terminus of HA1 and amino terminus of HA2 are separated by 22 Å in cleaved HA (Wilson et al., 1981). The prominent negative electrostatic charge of the cavity (red in Figure 3A) suggests the possibility that the newly cleaved positively charged N-terminal amino group may provide an electrostatic force to guide the docking of the fusion peptide. The existence of such an electrostatically charged cavity on the surface of HA0 suggests that a charged peptide or mimetic might bind in this pocket on HA0 and block the formation of the cleaved HA conformation and hence block infectivity. Following cleavage, at equilibrium, the covalently attached fusion peptides might be expected to saturate the pockets because of their high local concentration, but an inhibitor may still be effective if it

slowed the conformational rearrangement in Figures 2C and 2D. The transient, and unstable, intermediate following cleavage with the fusion peptide exposed might either aggregate or undergo an off-path conformational alteration, resulting in loss of activity.

Changes in pH have a different effect on HA0 than on cleaved HA due to the different environments of ionizable residues in the two structures (Figures 3C and 3D). Residues on the surface of the HA0 cavity exposed to solvent can change electrostatic charge at their appropriate pKa without affecting the fold of the protein; such surface charges are largely shielded by solvent and counterions. Once buried in HA, after cleavage of HA0, these ionizable residues (His-17 of HA1 and Asp-109 and -112) have the potential to disrupt the structure if they gain or lose protons. Examples from site-directed mutations of model proteins, where lysine was placed in a buried location in Staphylococcal nuclease, in a hyperstable mutant of Staphylococcal nuclease, and in lysozyme, all showed a strong pH dependence of protein stability, with the molecules becoming unstable as the lysine became charged at its depressed pKa (due to burial) near pH 6.0 (Dao-pin et al., 1991; Stites et al., 1991; Garcia-Moreno et al., 1997).

If we assume, for the sake of discussion, that the Asp-109, -112, and His-17 are not protonated in cleaved HA at pH 7.0 (if one is protonated at pH 7.0, it will have no effect when the pH is lowered), then lowering the pH could protonate them, depending upon their pKas in the buried environment of cleaved HA. Protonating the aspartic acids would eliminate some of their capacity as acceptors for hydrogen bonds (Figure 3D), but most of the hydrogen bonds would be preserved because even a protonated carboxylate can accept three hydrogen bond donors. If His-17 becomes protonated while completely buried by the fusion peptide in cleaved HA, the resulting buried positive charge might be destabilizing. The pKa for this buried histidine would be expected to be depressed. Once charged, the histidine, which up to then had been helping to hold HA together (Figures 3C and 3D), could be a strong force pushing it apart.

Mutant virus with Asp-112 (HA2) and His-17 (HA1) substitutions undergo the pH-induced conformational change at higher pH than wild-type, indicating a role for these residues in either stabilizing the neutral pH structure, triggering the low-pH-induced conformational change, or both (Daniels et al., 1985; Wiley and Skehel, 1987). Unfortunately, interpreting mutant data in this context is very uncertain. A single residue can have many roles in each conformation; e.g., in the X-ray structures of HA0 and cleaved HA, His-17 appears situated to stabilize HA0 at any pH and to stabilize cleaved HA above its pKa.

Other Viral Membrane Fusion Proteins

Recently, the structure of the cleaved conformation of the hemagglutinin-esterase-fusion glycoprotein (HEF) of influenza C virus has been determined by X-ray crystallography at neutral pH (Rosenthal et al., 1998; Zhang et al., submitted). Despite only 12% sequence identity with influenza A HA, the structures, especially in the HA2/HEF2 regions, are remarkably similar. Lysine 9 of HEF, homologous to His-17 in the HA amino acid sequence, is completely buried behind the fusion peptide of HEF in the cleaved HEF structure. Its ϵ-amino group makes only two hydrogen bonds with its noncharged neighbors, suggesting that it may be uncharged, with a depressed pKa similar to those in the model proteins discussed above (Dao-pin et al., 1991; Stites et al., 1991; Garcia-Moreno et al., 1997). The structure of uncleaved HEF (HEF0) is not known, so it is not known whether Lys-9 is on the surface of a cavity in that conformation.

Membrane fusion of many enveloped viruses is mediated by glycoproteins that are synthesized, folded, and oligomerize as a precursor that then must be cleaved to be activatable. In influenza virus, proteolytic cleavage of the envelope glycoprotein precursor HA0 primes the molecule for a subsequent low-pH-induced conformational change (Figure 4). The cleavage generates an apparently metastable cleaved HA conformation that low pH induces to refold into a conformation stable at both neutral and low pH, this low-pH-induced refolding event being required for membrane fusion. Other viruses, for example retroviruses like HIV-1, also synthesize an envelope glycoprotein gp160 that must be cleaved (gp120, gp41) to adopt a conformation that requires further structural changes before fusing membranes. In this case, the membrane-fusion conformational change is triggered by binding to receptor and in some cases coreceptor proteins, rather than low pH (Sattentau and Moore, 1991). It is likely that in these other cases, the precursor molecules will also contain surface cavities or features as in R329Q $HA0_s$ that will be occupied only after precursor cleavage and that may present targets on the precursor or during cleavage that might bind analogs of the fusion peptide to prevent the cleaved molecule from adopting a structure with membrane fusion potential.

Experimental Procedures

Protein Expression, Purification, and Characterization

Site-specific mutagenesis, cloning of mutated genes for HA into a vaccinia expression vector containing the cowpox p160 late promoter, and generation of recombinant vaccinia viruses were as described (Steinhauer et al., 1995).

Vaccinia-HA0 R329Q recombinant-infected CV-1 cells in 10 mM Tris (pH 8.0) were homogenized in a Dounce homogenizer. The suspension was made 70% w/v in sucrose, overlaid with 10 mM Tris (pH 8.0), and centrifuged for 2 hr at 25,000 rpm in a Beckman SW27. The membrane fractions separated by flotation were pelleted by centrifugation at 25,000 rpm for 60 min. Membranes resuspended in 10 mM Tris (pH 8.0), 10 mM calcium chloride, and 5 mM magnesium chloride (10^9 cell equivalents/10 ml) were incubated in 50 mg/ml trypsin (Sigma) and 1 U/ml DNase (Promega) at 37°C for 30 min. Membranes were pelleted by centrifugation at 50,000 rpm for 10 min in a Beckman TL100, and the supernatant was incubated with 25 mg/ml *C. perfringens* neuraminidase (Boehringer) at 37°C for 30 min. The mixture was then overlaid on a 10%–30% sucrose gradient in 10 mM Tris (pH 8.0) and centrifuged for 16 hr at 38,000 rpm in a Beckman SW41. Sucrose was removed from HA0-containing fractions during ultrafiltration through a Millipore PM10 membrane filter, and HA0 was further purified by binding to a Q15 Sartorius ion-exchange column in 10 mM Tris (pH 8.0) and eluting in 150 mM NaCl in 10 mM Tris (pH 8.0).

Crystallization and X-Ray Data Collection

R329Q $HA0_s$ crystals were grown in hanging drops from 15% PEG 4000, 75 mM NaCl, 50 mM HEPES (pH 7.5), and 0.1% NaN_3. Crystals

Table 1. Crystallographic Table

Data Statistics	
Space group	$I2_13$
Cell parameters	a = b = c = 153.0 Å $\alpha = \beta = \gamma = 90.0°$
Resolution limit	2.8 Å
Unique reflections	14,885
Completeness	99.8% (98%)[a]
R_{merge}	9.4% (36.8%)
Refinement Statistics	
Resolution range	8.0–2.8 Å
Number of reflections ($>2\sigma$)	13,933
R factor	22.4% (35.2%)
R_{free}	30.2% (35.5%)
Number of atoms (nonhydrogen)	4,070
Number of sugar residues	11
Rms deviations	
Bond length	0.009 Å
Bond angles	1.743°
Torsion angles	23.9°

[a] Statistics in 2.8–2.9 Å shell. $R_{free} = (\Sigma_h \mid Fo - Fc\mid)/(\Sigma_h Fo)$, $\forall h \in$ {free set}; $R_{work} = (\Sigma_h \mid Fo - Fc\mid)/(\Sigma_h Fo)$, $\forall h \in$ {working set}. $R_{merge} = (\Sigma_{hkl} \mid I - \langle I\rangle \mid)/(\Sigma_{hkl}\langle I\rangle)$, $\forall hkl \in$ {independent Miller indices}.

were harvested into solution also containing 17.5% PEG 4000 and prepared for flash cooling by serial transfers into a cryo-protecting solution of 25% MPD, 17.5% PEG 4000, and 50 mM HEPES (pH 7.5) at 4°C. Data were collected to 2.8 Å resolution with the Princeton 2K CCD detector at the F-1 beam line of the Cornell high energy synchrotron source (CHESS) and processed using DENZO and SCALEPACK (HKL Research) (see Table 1).

Structure Determination and Refinement

The structure was determined by molecular replacement using AMoRe (Navaza and Saludjian, 1997) and refined coordinates of a monomer of BHA, in which 25 residues around the cleavage site (residues 320–329 of HA1 and 1–15 of HA2) were omitted. One monomer of R329Q $HA0_s$ was found by a rotation and translation search with correlation coefficient 0.686 and R factor 35.2% using 10–3.5 Å data. The model was refined at 8–2.8 Å using X-PLOR (Brünger, 1992). The residues omitted in molecular replacement search were built into 2Fo-Fc, simulated annealing omit electron density maps by using MAIN (Turk, 1992). Simulated annealing omit maps were used extensively for building each residue in the cleavage loop 324–329 of HA1 and 1–15 of HA2. After the residues in the loop were placed approximately, the whole model was refined by iterative cycles of positional refinement (30–50 steps) in X-PLOR (Brünger, 1992) and manual refittings into 2Fo-Fc and Fo-Fc electron density maps by using MAIN and O (DATAONO AB). Grouped B factor and restrained individual B factor refinement (20 steps) were included at the final rounds of refinement. Despite the exposed nature of the cleavage loop and the high B factors (average from residue 323 to 12 is 70.0; overall average B = 35.0), continuous electron density for the main chain and most of the side chains was evident, with one break in the chain at Gly-4. No electron density was observed like that in a previously described pocket in HA2 (Skehel et al., 1982), which may be a consequence of the expression system or of some subtle structural distinction between R329Q $HA0_s$ and BHA. Ninety-five percent of the phi and psi angles are in the allowed regions of the Ramanchandran plot.

Acknowledgments

We acknowledge Dr. Anthony Planchart for initial contributions, and thank Kevin Booth for assistance; the staff at CHESS for help with data collection; and members of the Harrison/Wiley and Mill Hill research groups for useful discussions and assistance. The research was supported by the National Institutes of Health, the Medical Research Council (U.K.), and the Howard Hughes Medical Institute (HHMI). D. C. W. is an investigator of the HHMI.

Received July 24, 1998; revised September 2, 1998.

References

Bodian, D.L., Yamasaki, R.B., Buswell, R.L., Stearns, J.F., White, J.M., and Kuntz, I.D. (1993). Inhibition of the fusion-inducing conformational change of influenza hemagglutinin by benzoquinones and hydrobenzoquinones. Biochemistry *32*, 2967–2978.

Brünger, A. (1992). X-PLOR, Version 3.1: A System for X-Ray and NMR. (New Haven: Yale University Press).

Bullough, P.A., Hughson, F.M., Skehel, J.J., and Wiley, D.C. (1994). Structure of influenza haemagglutinin at the pH of membrane fusion. Nature *371*, 37–43.

Carr, C.M., and Kim, P.S. (1993). A spring-loaded mechanism for the conformational change of influenza hemagglutinin. Cell *73*, 823–832.

Carr, C.M., Chaudhry, C., and Kim, P.S. (1997). Influenza hemagglutinin is spring-loaded by a metastable native conformation. Proc. Natl. Acad. Sci. USA *94*, 14306–14313.

Chan, D.C., Fass, D., Berger, J.M., and Kim, P.S. (1997). Core structure of gp41 from the HIV envelope glycoprotein. Cell *89*, 263–273.

Chen, J., Wharton, S.A., Weissenhorn, W., Calder, L.J., Hughson, F.M., Skehel, J.J., and Wiley, D.C. (1995). A soluble domain of the membrane-anchoring chain of influenza virus hemagglutinin (HA2) folds in Escherichia coli into the low-pH-induced conformation. Proc. Natl. Acad. Sci. USA *92*, 12205–12209.

Collaborative Computational Project, Number 4. (1994). The CCP4 suite: programs for protein crystallography. Acta Crystallogr. D *50*, 760–763.

Daniels, R.S., Downie, J.C., Hay, A.J., Knossow, M., Skehel, J.J., Wang, M.L., and Wiley, D.C. (1985). Fusion mutants of the influenza virus hemagglutinin glycoprotein. Cell *40*, 431–439.

Dao-pin, S., Anderson, D.E., Baase, W.A., Dahlquist, F.W., and Matthews, B.W. (1991). Structural and thermodynamic consequences of burying a charged residue within the hydrophobic core of T4 lysozyme. Biochemistry *30*, 11521–11529.

Deshpande, K.L., Fried, V.A., Ando, M., and Webster, R.G. (1987). Glycosylation affects cleavage of an H5N2 influenza virus hemagglutinin and regulates virulence. Proc. Natl. Acad. Sci. USA *84*, 36–40.

Garcia-Moreno, E., Dweyer, J.J., Gittis, A.G., Lattman, E.E., Spencer, D.S., and Stites, W.E. (1997). Experimental measurement of the effective dielectric in the hydrophobic core of a protein. Biophys. Chem. *64*, 211–224.

Garten, W., Stieneke, A., Shaw, E., Wikstrom, P. and Klenk, H.-D. (1989). Inhibition of proteolytic activation of influenza virus hemagglutinin by specific peptidyl chloroalkyl detones. Virology *172*, 25–31.

Germino, J., and Bastia, D. (1984). Rapid purification of a cloned gene product by genetic fusion and site-specific proteolysis. Proc. Natl. Acad. Sci. USA *81*, 4692–4696.

Gething, M.J., Henneberry, J., and Sambrook, J. (1989). Fusion activity of the haemagglutinin of influenza virus. Curr. Top. in Membranes and Transport *32*, 337–364.

Godley, L., Pfeifer, J., Steinhauer, D., Ely, B., Shaw, G., Kaufmann, R., Suchanek, E., Pabo, C., Skehel, J.J., Wiley, D.C., and Wharton, S. (1992). Introduction of intersubunit disulfide bonds in the membrane-distal region of the influenza hemagglutinin abolishes membrane fusion activity. Cell *68*, 635–645.

Hanson, P.I., Roth, R., Morisaki, H., Jahn, R., and Heuser, J.E. (1997). Structure and conformational changes in NSF and its membrane receptor complexes visualized by quick-freeze/deep-etch electron microscopy. Cell *90*, 523–535.

Hay, A.J. (1989). The mechanism of action of amantadine and rimantadine against influenza viruses. In Concepts in Virus Pathogenesis, Volume III, A.L. Notkins and M.B.A. Oldstone, eds. (New York: Springer Verlag), pp. 361–367.

Hoffman, L.R., Kuntz, I.D., and White, J.M. (1997). Structure-based identification of an inducer of the low-pH conformational change in the influenza virus hemagglutinin: irreversible inhibition of infectivity. J. Virol. *71*, 8808–8820.

Kawaoka, Y., and Webster, R.G. (1989). Interplay between carbohydrate in the stalk and the length of the connecting peptide determines the cleavability of influenza virus hemagglutinin. J. Virol. *63*, 3296–3300.

Kawaoka, Y., Naeve, C.W., and Webster, R.G. (1984). Is virulence of H5N2 influenza viruses in chickens associated with loss of carbohydrate from the hemagglutinin? Virology *139*, 303–316.

Khatchikian, D., Orlich, M., and Rott, R. (1989). Increased viral pathogenicity after insertion of a 28S ribosomal RNA sequence into the haemagglutinin gene of an influenza virus. Nature *340*, 156–157.

Kido, H., Yokogoshi, Y., Sakai, K., Tashior, M., Kishino, Y., Fukutomi, A., and Kataunuma, N. (1992). Isolation and characterization of a novel trypsin-like protease found in rat bronchiolar epithelial Clara cells. A possible activator of the viral fusion glycoprotein. J. Biol. Chem. *267*, 13573–13579.

Klenk, H.-D., and Garten, W. (1994). Host cell proteases controlling virus pathogenicity. Trends Microbiol. *2*, 39–43.

Klenk, H.-D., and Rott, R. (1988). The molecular biology of influenza virus pathogenicity. Adv. Virus Res. *34*, 247–281.

Klenk, H.-D., Rott, R., Orlich, M., and Blodorn, J. (1975). Activation of influenza A viruses by trypsin treatment. Virology *68*, 426–439.

Klenk, H.-D., Angliker, H., Garten, W., Hallenberger, S., Ohuchi, M., Ohuchi, R., Shaw, S., Stieneke-Gröber, A., and Vey, M. (1993). Processing of viral glycoproteins by host proteases: structural aspects and functional consequences. In Virus Strategies, W. Doerfler and P. Böhm, eds. (Weinheim: Verlag Chemie), pp. 195–214.

Kraulis, J.P. (1991). MOLSCRIPT: a program to produce both detailed and schematic plots of protein structures. J. Appl. Crystallogr. *24*, 946–950.

Lazarowitz, S.G., and Choppin, P.W. (1975). Enhancement of the infectivity of influenza A and B viruses by proteolytic cleavage of the hemagluttinin polypeptide. Virology *68*, 440–454.

Maeda, T., and Ohnshi, S. (1980). Activation of influenza virus by acidic media causes hemolysis and fusion erthrocytes. FEBS Lett. *122*, 283–287.

Navaza, J., and Saludjian, P. (1997). AMoRe: an automated molecular replacement program package. Methods Enzymol. *276*, 581–594.

Nicholls, A., Bharadwaj, J., and Honig, B. (1991). GRASP: graphical representation and analysis of surface properties. Biophys J. *64*, 166–170.

Ohuchi, M., Orlich, N., Ohuchi, R., Simpson, B.E., Garten, W., Klenk, H.-D., and Rott, R. (1989). Mutations at the cleavage site of the hemagluttinin alter the pathogenicity of influenza virus A/chick/Penn/83 [H5N2]. Virology *168*, 274–280.

Orlich, M., Gottwald, H., and Rott, R. (1994). Nonhomologous recombination between the hemagglutinin gene and the nucleoprotein gene of an influenza virus. Virology *204*, 462–465.

Perdue, M.L., Garcia, M., Senne, D., and Fraire, M. (1997). Virulence-associated sequence duplication at the hemagglutinin cleavage site of avian influenza viruses. Virus Res. *49*, 173–186.

Rosenthal, P.B., Zhang, X., Formanowski, F., Fitz, W., Wong, C.-H., Meier-Ewert, H., Skehel, J.J., and Wiley, D.C. (1998). Three dimensional structure of the haemagglutinin-esterase-fusion glycoprotein of influenza C virus. Nature, in press.

Ruigrok, R.W., Aitken, A., Calder, L.J., Martin, S.R., Skehel, J.J., Wharton, S.A., Weis, W., and Wiley, D.C. (1988). Studies on the structure of the influenza virus haemagglutinin at the pH of membrane fusion. J. Gen. Virol. *69*, 2785–2795.

Sattentau, Q., and Moore, J.P. (1991). Conformational changes induced in the human immunodeficiency virus envelope glycoprotein by soluble CD4 binding. J. Exp. Med. *174*, 407.

Skehel, J.J., Bayley, P.M., Brown, E.B., Martin, S.R., Waterfield, M.D., White, J.M., Wilson, I.A., and Wiley, D.C. (1982). Changes in the conformation of influenza virus haemagglutinin at the pH optimum of virus-mediated membrane fusion. Proc. Natl. Acad. Sci. USA *79*, 968–972.

Steinhauer, D.A., Sauter, N.K., Skehel, J.J., and Wiley, D.C. (1992). Receptor binding and cell entry by influenza viruses. Semin. Virol. *3*, 91–100.

Steinhauer, D.A., Wharton, S.A., Skehel, J.J., and Wiley, D.C. (1995). Studies of the membrane fusion activities of fusion peptide mutants of influenza virus hemagglutinin. J. Virol. *69*, 6643–6651.

Stieneke-Grober, A., Vey, M., Angliker, H., Shaw, E., Thomas, G., Roberts, C., Klenk, H.-D., and Garten, W. (1992). Influenza virus hemagglutinin with multibasic cleavage site is activated by furin, a subtilisin-like endoprotease. EMBO J. *11*, 2407–2414.

Stites, W.E., Gittis, A.G., Lattman, E.E., and Shortle, D. (1991). In a staphylococcal nuclease mutant the side-chain of a lysine replacing valine 66 is fully buried in the hydrophobic core. J. Mol. Biol. *221*, 7–14.

Subbarao, K., Klimor, A., Katz, J., Reguery, H., Lim, W., Hall, H., Perdue, M., Swayne, D., Bender, C., Huang, J., et al. (1998). Characterization of an avian influenza A (H5N1) virus isolated from a child with a fatal respiratory illness. Science *279*, 393–395.

Tan, K., Liu, J., Wang, J., Shen, S., and Lu, M. (1997). Atomic structure of a thermostable subdomain of HIV-1 gp41. Proc. Natl. Acad. Sci. USA *94*, 12303–12308.

Turk, D. (1992). Weiterentwicklung eines programms fuer molekuelgraphik und elektrondichte-manipulation und seine anwendung auf verschiedene protein-strukturaufklaerungen. Ph.D. Thesis, Technische Universitaet, Muenchen.

Vey, M., Orlich, M., Adler, S., Klenk, H.D., Rott, R. and Garten, W. (1992). Hemagglutinin activation of pathogenic avian influenza viruses of serotype H7 requires the protease recognition motif R-X-K/R-R. Virology *188*, 408–413.

von Itzstein, M., Wu, W.Y., Kok, G.B., Pegg, M.S., Dyason, J.C., Jin, B., Van Phan, T., Smythe, M.L., White, H.F., and Oliver, S.W. (1993). Rational design of potent sialidase-based inhibitors of influenza virus replication. Nature *363*, 418–423.

Watowich, S.J., Skehel, J.J., and Wiley, D.C. (1994). Crystal structures of influenza virus hemagglutinin in complex with high-affinity receptor analogs. Structure *2*, 719–731.

Weber, T., Zemelman, B.V., McNew, J.A., Westermann, B., Gmachl, M., Parlati, F., Söllner, T.H., and Rothman, J.E. (1998). SNAREpins: minimal machinery for membrane fusion. Cell *92*, 759–772.

Webster, R.G., and Rott, R. (1987). Influenza virus A pathogeneticity: the pivotal role of hemagglutinin. Cell *50*, 665–666.

Weis, W., Brown, J.H., Cusack, S., Paulson, J.C., Skehel, J.J., and Wiley, D.C. (1988). Structure of the influenza virus haemagglutinin complexed with its receptor, sialic acid. Nature *333*, 426–431.

Weis, W.I., Cusack, S.C., Brown, J.H., Daniels, R.S., Skehel, J.J., and Wiley, D.C. (1990). The structure of a membrane fusion mutant of the influenza virus haemagglutinin. EMBO J. *9*, 17–24.

Weissenhorn, W., Dessen, A., Harrison, S.C., Skehel, J.J., and Wiley, D.C. (1997). Atomic structure of an ectodomain from HIV-1 gp 41. Nature *387*, 426–430.

WHO (World Health Organization). (1998). Weekly Epidemiological Record. *73*, 56–63.

Wild, C.T., Shugars, D.C., Greenwell, T.K., McDanal, C.B., and Matthews, T.J. (1994). Peptides corresponding to a predictive alpha-helical domain of human immunodeficiency virus type 1 gp41 are potent inhibitors of virus infection. Proc. Natl. Acad. Sci. USA *91*, 9770–9774.

Wiley, D.C., and Skehel, J.J. (1987). The structure and function of the hemagglutinin membrane glycoprotein of influenza virus. Annu. Rev. Biochem. *56*, 365–394.

Wilson, I.A., Skehel, J.J., and Wiley, D.C. (1981). Structure of the haemagglutinin membrane glycoprotein of influenza virus at 3 Å resolution. Nature *289*, 366–373.

Brookhaven Protein Data Bank ID Code

Coordinates for soluble R329Q mutant HA0 have been deposited in the Brookhaven Protein Data Bank under ID code 1ha0.